Available online: October 19, 2019

Commun. Fac. Sci. Univ. Ank. Ser. A1 Math. Stat.
Volume 69, Number 1, Pages 213–231 (2020)
DOI: 10.31801/cfsuasmas.544522
ISSN 1303–5991 E-ISSN 2618-6470
http://communications.science.ankara.edu.tr/index.php?series=A1

A SPACE-TIME DISCONTINUOUS GALERKIN METHOD FOR LINEAR HYPERBOLIC PDE'S WITH HIGH FREQUENCIES

ŞUAYIP TOPRAKSEVEN

Abstract. The main purpose of this paper is to describe a space-time discontinuous Galerkin (DG) method based on an extended space-time approximation space for the linear first order hyperbolic equation that contains a high frequency component. We extend the space-time DG spaces of tensor-product of polynomials by adding trigonometric functions in space and time that capture the oscillatory behavior of the solution. We construct the method by combining the basic framework of the space-time DG method with the extended finite element method. The basic principle of the method is integrating the features of the partial differential equation with the standard space-time spaces in the approximation. We present error analysis of the proposed space-time DG method for the linear first order hyperbolic problems. We show that the new space-time DG approximation has an improvement in the convergence compared to the space-time DG schemes with tensor-product polynomials. Numerical examples verify the theoretical findings and demonstrate the effects of the proposed method.

1. Introduction

In computational acoustics, the medium frequency regime and multiscale wave propagation governed by the wave equation have been gained a constant interest in last decades. When multiscale wave propagation presents a high frequency component, developing an efficient numerical methods for these classes of problem is a challenging task. Some example of high frequency problems include the high-intensity focused ultrasound (HIFU) treatment of cancer [1], coupled atomistic continuum modeling in nanomaterials [2] and tunneling in quantum mechanics [3]. The reason for inefficiency of the existing methods is that the standard numerical methods such as the finite element (FEM) or discontinuous Galerkin (DG) methods based on semi-discrete approach require a very fine mesh in the discretization

Received by the editors: March 25, 2019; Accepted: October 08, 2019.

2010 *Mathematics Subject Classification.* Primary 65M60,65M12,65M15; Secondary 35L03, 35L65.

Key words and phrases. Discontinuous Galerkin finite element methods, space-time discontinuous Galerkin methods, hyperbolic problems, high frequency solutions.

in both space and time, and this leads to huge computational cost and makes the numerical methods inefficient. Moreover, these methods based on semi-discrete approach may not suitable for multiscale approximations in the temporal domain. These issues on the standard numerical techniques have lead to high order methods that solve wave propagation phenomena in the time domain. One promising approach that has gained considerable popularity is space-time approximation spaces in which the time domain is also discretized. In these methods, two approaches have been proposed during the last decades. The first approach is called the time continuous space-time Galerkin methods (TCG) that do not require continuity in time. This approach generalizes the semi-discrete discretization to time domain with continuous time functions. The detailed explanations of such methods are given in [4]. The drawback of these methods is high computational cost because of discretization of whole domain. The second approach is based on space-time discontinuous Galerkin methods that use standard polynomials spaces to discretize the problem in space and time, while temporal domains are divided into time slab and discontinuities and jumps are allowed in time. In each slab, TCG method is applied and the next slab uses the information from the previous slab. This second approach is more robust and efficient than the first one. The wave equation can be discretized by a space-time setting in two ways. One way is to discretize the wave equation directly in a one field formulation with only one unknown as [5] and [6] . The second way is to convert the second order equation to a system of first order equations as done in [7] and [8]. Using this second formulation, a *priori* and a *posteriori* error estimates have been proved in [9] using linear interpolation. This approach clearly increases the unknowns in the resulting systems. Error estimates to prove convergence of the methods have been derived by French [6] and Hughes and Hulbert [5]. In the latter work, Galerkin least-squares stabilization terms are added for convergence analysis. In [6], the weighted inner product is included for the stability. A space-time DG method in which discontinuities and jumps are allowed both in space and time have been developed in [10] and recently proposed in [11] and [12] with discontinuous Petrov-Galerkin method in temporal domain for linear hyperbolic systems. Furthermore, many applications require boundary movement such as Stefan problems and water waves. In such problems, the mesh points also move in order to capture boundary movement. These movements in mesh points make the numerical scheme in efficient or need more complicated numerical discretization. In this case, it is natural to consider the space-time discontinuous Galerkin approach. Analysis and survey of space-time DG method for hyperbolic and parabolic conservation laws on time dependent domains are explained in details in [13]. Recently, space-time methods have become popular for the time dependent problems discussed in [14] and [15]. An application of this method to the compressible Vaiver-Stokes equations is discussed in [17]. Space-time DG method for the advection-diffusion equation has been given in details in [18] and [19]. This method also has been successively applied to nonconservative hyperbolic PDEs as models for dispersed multiphase flows in [20]. Furthermore, space-time DG methods have been proposed for the nonlinear water waves in [21] as well.

The medium or high frequency in wave propagation has been dealt with high order numerical methods including the ultra-weak variational method [22] that is a special case of the Trefftz-DG formulation for the wave equation [23] and the discontinuous enrichment method [24]. In these methods, the approximation space is enriched by the solution of the equation under consideration. In [24], the DG space is extended by solutions of the homogeneous differential equation that capture the high frequency in the solutions. In the same direction, an enriched space-time FEM for the first-order hyperbolic systems with discontinuities in both space and time has been studied by Chessa and Belytschko [25]. This enriched space-time approach is based on the extended FEM studied in [26]. These methods are based on the partition of unity approach developed in [27]. Motivated by these approaches, in this paper we propose a high-order accurate space-time DG method that is well-suited for first order linear hyperbolic problem with high frequency components. We construct the extended space-time DG space by enriching space-time DG space with the trigonometric functions in space and time. These trigonometric-function spaces intuitively capture the high frequency solutions and should be used to the highly oscillatory problems. This extended space time DG method is an extension to an extended DG method presented in [28]. We will show global convergence in error estimates. Our error analysis based on the DG method proposed by [29].

The outline of this paper is as follows: Section 2 describes the mathematical analysis, formulations, and an introduction to a space-time DG method for scalar hyperbolic linear equation with high-frequency components. The basic properties of the proposed space-time DG method, the geometry of the space-time domain and elements and the space-time formulation of the problem have been explained and discussed and general solution form for linear hyperbolic equation with high frequency components is also given in Section 2. In Section 3, we introduce preliminaries and notations and recall some basic facts on DG methods for linear hyperbolic equations. We present our extended DG method for linear hyperbolic equation with high frequency components and our special interpolation operators have been given in Section 4. Stability and error analysis are given in Section 5. In Section 6 numerical example is given to show that our theoretical results agree with numerical results. Finally we explain some conclusion and future direction in Section 7.

2. Space-Time Formulation with Trigonometric Functions

The basic principle of an extended DG method is to enrich the DG space by special functions that are, generally, the solution of homogeneous differential equation. The linear hyperbolic equation has the solution of the form $h(x \pm t)$ in one dimension. In Section 2.2, we show that if the initial condition has a high frequency component, then the homogeneous differential equation will also have a high frequency functions. This observation suggests that the enrichment shape functions consist of the polynomials and the trigonometric functions in the space $E := span\{\sin(x \pm t), \cos(x \pm t)\}$. A similar idea has been proposed for the wave equation in [30] and Trefftz DG method in [23].

2.1. **Problem Statement.** In this paper, we consider a scalar hyperbolic equation in an open domain Ω with boundary $\partial\Omega$

$$\text{Find } U = U(x,t) \text{ so that}$$
$$\begin{cases} \mathcal{L}U(x,t) + c(x,t)U(x,t) = g(x,t) \quad \text{on } Q_T, \quad 0 < c_0 \le c \le c_1, \\ U(x,0) = f(x). \end{cases} \tag{1}$$

Here, $\mathcal{L}U := \frac{\partial U}{\partial t} + \gamma \frac{\partial U}{\partial x}$, $Q_T = \Omega \times (0,T]$ and c_0 and c_1 are constants with $\gamma \in (0,1]$ and U denotes a scalar quantity, and t represents time with T the final time. This problem has been chosen purely for its simplicity. This analysis can be easily extended to more general hyperbolic and scalar conservation law problems.

We propose a space-time DG method based on extended DG approximation space for the equation (1). In this method, we directly consider the domain $Q_T \subset \mathbb{R}^2$ in which spatial and temporal variables are not distinguished and a point $\hat{x} \in Q_T$ has coordinates (x_0, x_1) with $x_0 = t$ representing a time variable and $x = x_1$ space variable. Thus, we define the space-time domain as the open domain $Q_T \subset R^2$. For space-time discretization, we need space-time slabs and elements. To do this, we partition the time interval $I = (0,T]$ into an ordered time levels $0 = t_0 < t_1 < \cdots < t_N = T$. Let $I_n = (t_n, t_{n+1})$ so that $I = \cup_n I_n$ with the time length $\Delta t = t_{n+1} - t_n$. Let $\Omega(t_n)$ denote the space-time domain at the time level $t = t_n$. Then, we define space-time slabs as $Q_T^n = Q_T \cap I_n$. We divide further $\Omega(t_n)$ into non-overlapping spatial elements K^n and similarly we divide the spatial domain $\Omega(t_{n+1})$ into elements K^{n+1}. We then connect the elements K^n and K^{n+1} to obtain space-time element $\mathcal{K}^n$ by using linear interpolation in time. We also describe the tessellation of the space-time slab $T_h^n = \cup_n \mathcal{K}^n$ and all space-time elements $T_h = \cup_n T_h^n$ in Q_T. By $\partial\mathcal{K}$ we denote the boundary of the space-time element $\mathcal{K}$. These space-time elements can be mapped to reference element (square or rectangle) by a suitable map, e.g., see [13] for construction of such a map. Figure 1 show a sketch of the space-time slab in Q_T.

In this paper, we require c and g are slowly varying smooth functions with bounded derivatives of many orders while f has the high frequency components. For instance, if $f(z) = cos(\omega z)$, then the solution has the form of:

$$U(x,t) = S(x,t) + R(x,t)\cos\big(\omega(x-t)\big), \tag{2}$$

where the frequency ω is a large number in absolute value. We further assume the functions $S(x,t)$ and $R(x,t)$ are slowly-varying functions of x and t in the sense that they have many derivatives all of which have norms that are moderately sized in space.

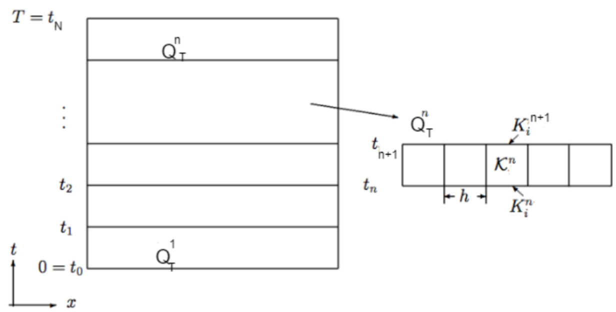

FIGURE 1. Space-time slab in space-time domain Q_T. On the right, the rectangular mesh is an example of structured discretizations in space and time.

We can assume that the forcing term $g(x,t)$ has also frequency components and we can show a similar solution form to (2). However, in this case extending the DG space with trigonometric functions is not easy task since we should extend the approximation space in all characteristic lines. For example, if we let $g(x,t) = \sin(\beta x) + \cos(\eta t)$ with $\beta, \eta >> 1$, then the solution form looks like $U(x,t) = S_1(x,t)\sin(\beta(x-t)) + S_2(x,t)\cos(\eta t) + R(x,t)\cos(\omega(x-t))$ so that S_1, S_2 and R do not have high frequency component. Therefore, enriching the space-time DG space is not easy job in this simple example. As an application of this phenomena, we consider high-intensity focused ultrasound (HIFU) treatment of cancer that uses sound wave. Tumors in body tissues are destroyed when HIFU is focused onto them. The initial condition in partial differential equation will generally help to determine high frequency shape to destroy tumor. In Figure 2, high frequency components in the initial condition determine acoustic pressure (high frequency shape) that heats and destroys the tumor.

We define an interpolation based on the assumption (2) in the error analysis of the proposed method. Hence, we prove this assumption in the next subsection.

2.2. **General Form of the Solutions.** In this section, we give the explicit solution form of the following problem:

$$\begin{cases} \text{Find } U = U(x,t) \text{ on } \mathbb{R} \times [0,T] \text{ so} \\ \quad \partial U/\partial t + \partial U/\partial x + cU = g \qquad 0 < c_0 \le c(x,t) \le c_1, \\ \text{with } U(x,0) = f(x). \end{cases} \tag{3}$$

The variable change to characteristic lines helps transform the PDE to an infinite set of ODE's. Let $x = t + x_0$ where $x_0 \in \mathbf{R}$ and define

$$\tilde{U}(t) = U(t + x_0, t).$$

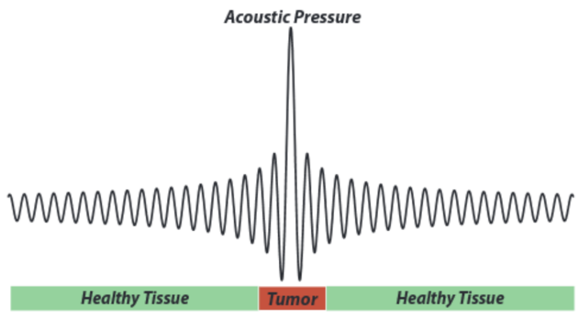

FIGURE 2. High frequency sound waves are concentrated on body tissues and tumor heats up and dies.

Then, we find that

$$\tilde{U}' = U_t + U_x = -cU + g,$$

or, with $\tilde{C}(t) = c(t + x_0, t)$ and $\tilde{G}(t) = g(t + x_0, t)$ we have

$$\tilde{U}' + \tilde{C}\tilde{U} = \tilde{G} \quad \text{and} \quad \tilde{U}(0) = f(x_0).$$

We multiply this equation by an integrating factor $\tilde{\mu}$ and find

$$\tilde{\mu}(t) = \exp\left(\int_0^t \tilde{C}(s)\ ds\right) \quad \Rightarrow \quad \left(\tilde{\mu}(t)\tilde{U}(t)\right)' = \tilde{\mu}(t)\tilde{G}(t).$$

This first order linear BVP (in $\tilde{U}$) can now be solved and we find that

$$\tilde{U}(t) = \frac{1}{\tilde{\mu}(t)}\left(f(x_0) + \int_0^t \tilde{\mu}(s)\tilde{G}(s)\ ds\right).$$

So, now we unwind the variable change to produce a solution for U. Note that $x_0 = x - t$ and, thus, letting

$$\mathcal{I}(x,t) = 1/\tilde{\mu}(t) = \exp\left(-\int_0^t c(s + (x-t), s)\ ds\right),$$

we have

$$U(x,t) = f(x-t)\mathcal{I}(x,t) + \mathcal{I}(x,t)\int_0^t \mathcal{I}(x,s)g(s + (x-t), s)\ ds.$$

If we now assume that g and c are slowly varying smooth functions with bounded derivatives of many orders while f has the high frequency components; that is, say,

$$f(z) = \cos(\omega z) \quad \text{for } \omega >> 1,$$

then, we have

$$U(x,t) = S(x,t) + R(x,t)\cos(\omega(x-t)).$$

This proves the assumption (2).

3. Preliminaries and Notations

The Sobolev space, $W^{m,p}(K)$, for a domain K, consists of functions with m derivatives in the $L^p(K)$ norm. We will use the following notation for Sobolev space semi-norms and norms for $1 \le p < \infty$

$$|v|_{m,p,K} = \left(\sum_{|\alpha|=m} \|D^\alpha v\|^p_{L^p(K)} \right)^{1/p} \quad \text{and} \quad \|v\|_{m,p,K} = \left(\sum_{|\alpha|\le m} \|D^\alpha v\|^p_{L^p(K)} \right)^{1/p}, \tag{4}$$

and when $p = \infty$

$$\|v\|_{m,\infty,K} = \sum_{|\alpha|\le m} \|D^\alpha v\|_{L^\infty(K)}, \tag{5}$$

where $D^\alpha v = \dfrac{\partial^{|\alpha|} v}{\partial x_1^{\alpha_1} \dots \partial x_n^{\alpha_n}}$ with $|\alpha| = \sum_{k=1}^n \alpha_k$ for $\alpha_k \ge 0, \quad k = 1, \dots, n$, and $x^\alpha = x_1^{\alpha_1} \dots x_n^{\alpha_n}$ and the standard Lebesgue space $L^p(K)$ norms

$$\|v\|_{L^p(K)} = \Big(\int_K |v|^p \, dx \Big)^{1/p} \quad \text{for} \quad 1 \le p < \infty,$$

and

$$\|u\|_{L^\infty(K)} = ess\, sup_{x\in K} |v(x)|.$$

For simplicity, we occasionally denote $\|.\|_{0,2,K}$ by $\|.\|$.

We will primarily be working with the Hilbert space $H^m(K) = W^{m,2}(K)$.

Let $P_r(K)$ be the space of polynomials with degree $\le q$ in K. We also assume there is an interpolation operator [[31], Theorem 4.4.4]

$$\pi_h : W^{q+1,p}(K) \to P_r(K)$$

for which

$$\|(I - \pi_h)v\|_{\ell,p,K} \le Ch^{r-\ell} \|v\|_{r,p,K}, \qquad (0 \le \ell \le r \le q+1). \tag{6}$$

and $\pi_h \xi = \xi$ for $\xi \in P_r(K)$. Moreover, if $v \in C(\bar{\Omega})$ then $\pi_h v$ is continuous on $\bar{\Omega}$ as well.

The inverse inequality [[31], Theorem 4.5.11] for functions $\chi \in P_r(K)$ states that there exists $C > 0$, which is independent of h, so that

$$\|\chi\|_{\ell,p,K} \le Ch^{m-\ell+1/p-1/r} \|\chi\|_{m,r,K}, \quad m \le \ell, \quad 1 \le p \le \infty, \quad \text{and} \quad 1 \le r \le \infty. \tag{7}$$

The *arithmetic-geometric mean* inequality states that for scalars a and b,

$$|ab| \le \delta a^2 + C_\delta b^2, \tag{8}$$

where $C_\delta = 1/(4\delta)$ and $\delta > 0$.

To be able to easily present our results and compare with previous works, we follow the paper by C. Johnson and J. Pitkaranta [29]. Given a piecewise smooth function v write $v^n(.) = v^-(., nh)$ and the approximate solution u is computed successively on the strips $S_n = \{x \in \Omega : (n-l)h < t < nh\}, n = l, ..., N$ so that $\|u^n - U^n\|$ is the error on each time level $t = nh$.

Let $n_K = (n_x^K, n_t^K)$ represent the outward pointing unit normal vector on ∂K with space coordinate n_x^K and the time coordinate n_t^K. Let $\beta := (1, \gamma)$ and $\partial Q_T := \Gamma$. The inflow boundary is defined

$$\Gamma\_ := \{\hat{x} \in \Gamma : n_K \cdot \beta < 0\} = \{(x,t) : x = 0 \quad \text{or} \quad t = 0\}.$$

In an element K, its inflow boundary $\partial K\_$ and its outflow $\partial K_+ = \partial K \backslash \partial K\_$ is similarly defined by

$$\partial K\_ = \{x \in \partial K : n_K \cdot \beta < 0\},$$
$$\partial K_+ = \{x \in \partial K : n_K \cdot \beta > 0\}.$$

Space-time DG space is then defined as

$$V_h := \{v \in L_2(Q_T) : v|_K \in P_r(K), \quad \forall K \in T_h\}. \tag{9}$$

where $P_r(K)$ denotes the space of polynomials of maximum degree at most r in (x,t). Functions in V_h are allowed to be discontinuous at discrete time level. For $K \in T_h$, and a piecewise smooth function v, we define the jump operator by

$$[u](x) = \lim_{s \to 0^+} \big(u(x+s) - u(x-s)\big)$$

when $x \in \partial K\_ \subset \mathcal{E}$, interior faces, and $[u](x) := u(x)$ when $x \in \Gamma\_ \cap \partial K\_$. The jump of v across $\partial K\_ \backslash \Gamma$ defined similarly by

$$[v]_K := v_K^+ - v_K^-,$$

where v_K^+ the trace of v on ∂K taken from within the element K and v_K^- is the exterior trace of u. Note that the sign of the jump depends on the direction of the flow. The average of a function u is defined by

$$\{u\} = \frac{1}{2}(u|_{K_1} + u|_{K_2}) \qquad \text{on} \quad \partial K_1 \cap \partial K_2.$$

We define the equivalent space-time DG method for (1) by summing over $K \in T_h$: Find $u \in V_h$ so that

$$a(u,v) = \ell(v), \qquad \forall v \in V_h, \tag{10}$$

where

$$a(u,v) = \sum_K \big((\mathcal{L}u + cu, v)_K - \langle [u], v^+ \rangle_{\partial K\_}\big), \tag{11}$$

and

$$\ell(v) = (g,v), \qquad \langle u, v \rangle_{\partial K} = \int_{\partial K} |n_K \cdot \beta| uv \, ds. \tag{12}$$

where $\beta = (1, \gamma)$ and n_K is the outward unit normal to ∂K.

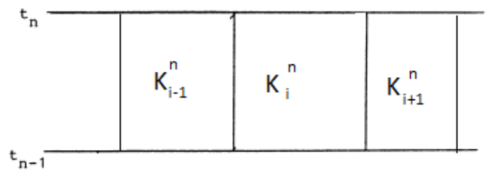

FIGURE 3. The order of the space-time elements on which u is computed.

Note that, for differentiable functions u and v, we have the following integration by parts formula

$$(\mathcal{L}u, v)_K = -(u, \mathcal{L}v)_K + \langle u, v\rangle_{\partial K_+} - \langle u, v\rangle_{\partial K_-}.$$

Equivalently, using this formula we may write this as

$$a(u, v) = \sum_K (-(u, \mathcal{L}v + cv)_K - \langle u^-, [v]\rangle_{\Gamma_h} + \langle u, v\rangle_{\Gamma_+}, \tag{13}$$

where $\Gamma_h := \Big(\bigcup_K \partial K\Big)\backslash\Gamma$.

Now, we have the Galerkin orthogonality relation by replacing u by the exact solution U in (11)

$$a(u - U, v) = 0, \quad \forall v \in V_h. \tag{14}$$

Let us recall the DG method for (1). Given a finite element partitioning $\mathcal{J}_h := \{K\}$ of Q_T, we look for a solution u defined on Q_T such that for all $K \in \mathcal{J}_h$ and $u|_K \in P_r(K)$ so that

$$\int_K (\mathcal{L}u + cu)v dx + \int_{\partial K_-} M_K [u]_K v^+ \, ds = (g, v)_K \quad \forall v \in P_r(K), \tag{15}$$

where $M_K := |n_K.\beta|$.

As shown in [29], u is uniquely determined by (15) and it is possible to compute u successively on each K starting at the inflow boundary Γ_- where u is given. Then it is possible to find the numerical solution u successively on one time level after another computing space-time element by element by starting for each strip on the left. The order of elements on which u will be computed is shown in Figure 3. Thus, given g and u^- on inflow boundary, we can solve u locally in each K as shown below. For detailed proof, we refer the reader to [29].

Below, we denote by C , a positive constant which may take different values on different occurrences.

Lemma 1. [29] *Assume that $g \in L_2(Q_T)$ and $f \in L_2(\Gamma_-)$ are given in (1). Then u is determined by (15) and the following local stability holds for each K*

$$\|u\|_K + h^{\frac{1}{2}}\|u^+\|_{\partial K_-} + h^{\frac{1}{2}}\|u^-\|_{\partial K_+} \le C\{h\|g\|_K + h^{\frac{1}{2}}\|M_K u^-\|_{\partial K_-}\}.$$

Let us introduce a norm $|||.|||_h$ for the error analysis :

$$|||u|||_h^2 = \sum_K h||\mathcal{L}u||_K^2 + |u|_h^2.$$

$$|u|_h^2 = ||u||^2 + \frac{1}{2}\big\langle [u], [u] \big\rangle_{\partial K_-} + \frac{1}{2}\big\langle u^-, u^- \big\rangle_{\Gamma_+},$$

$$|||u|||_h^2 = \sum_K h||\mathcal{L}u||_K^2 + |u|_h^2.$$

Then, we have the following a generalization of the *Poincare-Friedrichs* inequality [31]:

$$\forall w \in H^1(K), \quad \|w\|_{0,2,Q_T} \le C|||w|||_h. \tag{16}$$

4. Space-time Discontinuous Galerkin Discretization

In this section, we discuss the space-time DG method based on the extended space-time approximation spaces and that combines the framework of space-time DG with XFEM for the linear hyperbolic equation. We enrich the space-time DG space by adding a range of Fourier-series components to handle the high-frequency terms in the exact solution. As shown in Section 2.1, if the initial condition has only one high frequency component, then the solution form given by (2). In the same direction, if we assume that the initial condition has L high frequency components, that is, $f(z) = \sum_{\ell=1}^{L} \cos(\omega_\ell z)$ with $\omega_\ell >> 1$, then we wil have the solution form of

$$U(x,t) = S(x,t) + \sum_{\ell=1}^{L} R(x,t)\cos(\omega_\ell(x-t)). \tag{17}$$

Thus, our "enriched space" $X_h^r(Q_T)$ consists of the functions of the form

$$X_h^r(Q_T) = \{\psi = s + \sum_{\ell=1}^{L} (a_\ell \text{cos}(n_\ell(x-t)) + b_\ell \text{sin}(n_\ell(x-t)))\}, \tag{18}$$

where $n_1, \ldots, n_L$ are integers and s as well as the a_i's and the b_i's are all elements of the space-time DG space V_h (9). More precisely, these s, a_ℓ and b_ℓ functions are tensor-product of piecewise discontinuous polynomials of degree at most r in x and t variables. Note that these functions are allowed to be discontinuous at the nodal points both in space and time and continuous in each element. This enriched space provides good approximations to the solutions of (1) if the range of high frequencies are known *a priori*.

For a high-frequency component of (17), we have, by using a simple trigonometric identities,

$$\begin{aligned} R(x,t)\cos(\omega_\ell y) &= R(x,t)\cos(n_\ell y + (\omega_\ell - n_\ell)y) \\ &= R(x,t)\,\cos((\omega_\ell - n_\ell)y)\,\cos(n_\ell y) - R(x,t)\,\sin((\omega_\ell - n_\ell)y)\,\sin(n_\ell y), \end{aligned}$$

where $y := x - t$ and n_ℓ is an integer and can be chosen between n_0 and n_L with $0 \le \omega_\ell - n_\ell \le 1$. The key idea is that the functions

$$\alpha_\ell(x,t) = R(x,t)\,\cos((\omega_\ell - n_\ell)(x-t)),$$

and

$$\beta_\ell(x,t) = -R(x,t)\,\sin((\omega_\ell - n_\ell)(x-t))$$

oscillate slowly since their frequencies are small and can be well approximated by functions in V_h.

We now directly approximate the form (2) using interpolation. Let

$$U_A(x,t) = \pi_h S(x,t) + \sum_{\ell=n_0}^{n_L} \left[(\pi_h\alpha_\ell)(x,t)\cos(n_\ell(x-t)) + (\pi_h\beta_\ell)(x,t)\sin(n_\ell(x-t))\right]. \tag{19}$$

Note that $U_A \in X_h^r(Q_T)$ and we have

$$\begin{aligned} U(x,t) - U_A(x,t) = (I-\pi_h)S(x,t) + \sum_{\ell=n_1}^{n_\ell} \Big[&(I-\pi_h)\alpha_\ell(x-t)\cos(n_\ell(x-t)) \\ &+ (I-\pi_h)\beta_\ell(x-t)\sin(n_\ell(x-t))\Big]. \end{aligned}$$

So, using (6), there is constant C, independent of h and ω_ℓ, we have

$$\|U - U_A\|_{m,p,K} \le C h^{r+1-m}\omega_L^m, \qquad 0 \le m \le p \le r+1. \tag{20}$$

Also, since U is continuous, it follows that U_A is continuous as well.

We remark that if $U \in P_r(Q_T)$, that is U is a polynomials, then our special interpolation agrees with the interpolation operator π_h so that in this case we have

$$U_A = \pi_h U. \tag{21}$$

Furthermore, we have, by the trace inequality,

$$\|U - U_A\|_{0,2,\partial K} \le C h,^{r+\frac{1}{2}} \qquad 0 \le m \le 2 \le r+1. \tag{22}$$

To construct our space-time approximation solution on the extended space, we perform the space-time discretization of the linear hyperbolic equation (1). Thus, we define the space-time DG scheme : Find $u \in X_h^r$ so that

$$a(u,v) = \ell(v) \quad \forall v \in X_h^r. \tag{23}$$

First, we show that the discrete problem (23) is stable from which the existence and uniqueness of the problem follows. Then we prove the bilinear form $a(.,.)$ is coercive and continuous. For short reference, we take $M_K = M$.

Lemma 2. *The solution u to the problem (23) satisfies the following stability estimates*

$$|||u|||_h^2 \leq C\big(\|g\|^2 + \|Mf\|_{\Gamma_-}^2\big). \tag{24}$$

Proof. Taking $v = u + \delta\mathcal{L}u$ when $\delta = Ch$ for some constant C in (23) we have, for each $K \in T_h$

$$a(u, u + \delta\mathcal{L}u) = (\mathcal{L}u + cu, u + \delta\mathcal{L}u) - \int_{\partial K_-} [u]u^+ M\, ds = (g, u + \delta\mathcal{L}u)_K. \tag{25}$$

Now, using Green's formula we have

$$2(\mathcal{L}u, u) = \int_{\partial K_+} (u^-)^2 M\, ds - \int_{\partial K_-} (u^+)^2 |M|\, ds,$$

and since $c \geq c_0 > 0$, we get

$$2a_K(u, u + \delta\mathcal{L}u) \geq 2\delta(\mathcal{L}u, \mathcal{L}u)_K + 2c_0(u, u)_K + (1 + \delta c_0)\Big(\int_{\partial K_+} (u^-)^2 M\, ds - \int_{\partial K_-} (u^+)^2 |M|\, ds\Big) + 2\int_{\partial K_-} [u]u^+ |M|\, ds.$$

Since every side of interior element boundary ∂K_+ agrees with a side of $\partial K'_-$ for an neighbour element K', we have

$$\sum_K \int_{\partial K_+} (u^-)^2 M\, ds = \sum_K \int_{\partial K_-} (u^-)^2 |M|\, ds + \int_{\Gamma_+} (u^-)^2 M\, ds + \int_{\Gamma_-} (u^-)^2 M\, ds, \tag{26}$$

and consequently if we take $\delta = Ch$ for some constant C with $h \leq 1$ and using the fact that $1 + Ch \geq 1$

$$2a(u, u + Ch\mathcal{L}u) \geq 2Ch \sum_K (\mathcal{L}u, \mathcal{L}u)_K + 2c_0 \sum_K (u, u)_K + \sum_K \int_{\partial K_-} \Big(\big((u^+)^2 - 2u^+u^- + (u^-)^2\big)|M|\, ds\Big) + \int_{\Gamma_+} (u^-)^2 M\, ds - \int_{\Gamma_-} (u^-)^2 |M|\, ds.$$

Thus we obtain

$$a(u, u + Ch\mathcal{L}u) \geq Ch \sum_K \|\mathcal{L}u\|^2 + c_0\|u\|^2 + \frac{1}{2}\sum_K \int_{\partial K_-} [u]^2 |M|\, ds + \frac{1}{2}\int_{\Gamma_+} (u^-)^2 M\, ds - \frac{1}{2}\int_{\Gamma_-} (u^-)^2 |M|\, ds. \tag{27}$$

Now we estimate the right-hand side of (25). Applying the Cauchy-Schwarz and the arithmetic-geometric inequalities we get

$$(g, u + Ch\mathcal{L}u) \leq \|g\|^2 + \frac{1}{4}\|u\|^2 + \frac{Ch}{4}\sum_K \|\mathcal{L}u\|_K^2. \tag{28}$$

Using the fact that $u_\_ = f$ on $\Gamma_\_$ and combining (27) and (28), the desired result follows. □

In particular this estimate shows the uniqueness and existence of a solution to (23)

Now we prove the improved stability estimate.

Lemma 3. *The following improved stability holds for $\delta = Ch$ with suitable constant C*

$$a(u, u + \delta\mathcal{L}u) \geq C\Big(|||u|||_h^2 - \int_{\Gamma_\_} (u^-)^2|M|\,ds\Big). \tag{29}$$

Proof. From (27) and the definition of the norm (3) , the result easily follows. □

5. Error Analysis of the Space-time DG Method

We can now state and prove the basic global error estimate for our space-time DG method (23).

Theorem 4. *If u satisfies (23) and U satisfies (1), then we have the following error estimate*

$$|||e|||_h \leq C\omega h^{r+\frac{1}{2}}, \tag{30}$$

where C does not depend on ω and h.

Proof. Let $U_A \in X_h^r$ be the special interpolation of U defined by (19). Let us write

$$\eta := U - U_A, \qquad \theta := u - U_A, \quad e = \theta - \eta.$$

Using Lemma 3 with $u = e$ and $\delta = Ch$ and the orthogonality property (14) with $v = \theta$ and the fact that $e_\_ = 0$ on $\Gamma_\_$, we have

$$C|||e|||_h^2 \leq a(e, e + Ch\mathcal{L}u) = a(e, e) + Cha(e, \mathcal{L}\eta) := T_1 + T_2. \tag{31}$$

In order to bound T_1, we first prove that

$$a(e, e) = |e|_h^2. \tag{32}$$

By Green's formula for each K

$$2(\mathcal{L}e, e)_K = \int_{\partial K_+} (e^-)^2 M\,ds - \int_{\partial K_\_} (e^+)^2|M|\,ds,$$

and thus

$$2a(e, e) = \sum_K \Big\{ \int_{\partial K_+} (e^-)^2 M\,ds - \int_{\partial K_\_} (e^+)^2|M|\,ds + 2\int_{\partial K_\_} (e^+ - e^-)e^+|M|\,ds\Big\} + 2\|e\|^2.$$

Now using the identity (26) with $u = e$ along with the fact that $e^- = 0$ on $\Gamma\_$ we obtain that

$$2a(e,e) = \sum_K \Big\{ \int_{\partial K_-} \big((e^+)^2 - 2e^+e^- + (e^-)^2\big)|M|\, ds \Big\} + \int_{\Gamma_+} (e^-)^2 M\, ds + 2\|e\|^2,$$

which proves the result (32).

We next bound the term T_2. To end this, we bound the bilinear form $a(e, \mathcal{L}\eta)$. So using the Cauchy-Schwarz and the arithmetic-geometric inequalities we have

$$\begin{aligned} a(e,\mathcal{L}\eta) &= \sum_K \Big\{ \big(\mathcal{L}e + ce, \mathcal{L}\eta\big)_K - \int_{\partial K_-} [e]\eta^+ M\, ds \Big\} \\ &\le \frac{1}{2}\sum_K \|\mathcal{L}e\|_K^2 + \frac{1}{2}\|\mathcal{L}\eta\|^2 + \frac{h^{-1}}{2}\|e\|^2 + \frac{h}{2}\|\mathcal{L}\eta\|^2 \\ &\quad + \sum_K \Big(\frac{1}{4h}\int_{\partial K_-} [e]^2 |M|\, ds + h\int_{\partial K_-} \eta^2 |M|\, ds \Big), \end{aligned}$$

thus we find that

$$\begin{aligned} Cha(e,\mathcal{L}\eta) &\le \frac{h}{2}\sum_K \|\mathcal{L}e\|_K^2 + \frac{h}{2}\|\mathcal{L}\eta\|^2 + \frac{1}{2}\|e\|^2 + \frac{h^2}{4}\|\mathcal{L}\eta\|^2 \\ &\quad + \sum_K \Big(\frac{1}{4}\int_{\partial K_-} [e]^2 |M|\, ds + h^2\int_{\partial K_-} \eta^2 |M|\, ds \Big), \end{aligned}$$

and

$$Cha(e,\mathcal{L}\eta) \le \frac{1}{2}|||e|||_h^2 + \frac{h}{2}\|\mathcal{L}\eta\|^2 + \frac{h^2}{4}\|\mathcal{L}\eta\|^2 + \sum_K h^2 \int_{\partial K_-} \eta^2 |M|\, ds.$$

Using the bounds (20) and (22) and the fact that the number of elements is $O(h^{-2})$ we can bound the right hand-side by

$$\begin{aligned} Cha(e,\mathcal{L}\eta) &\le \frac{1}{2}|||e|||_h^2 + \frac{h}{2}C\omega^2 h^{2r} + \frac{h^2}{4}C\omega^2 h^{2r} + \sum_K h^2 C h^{2r+1} \\ &\le \frac{1}{2}|||e|||_h^2 + C\omega^2 h^{2r+1} + C\omega^2 h^{2r+2} + Ch^{-2}h^2 h^{2r+1} \\ &\le \frac{1}{2}|||e|||_h^2 + C\omega^2 h^{2r+1}. \end{aligned} \tag{33}$$

Finally inserting (32) and (33) into (31), it follows that

$$|||e|||_h^2 \le C\omega^2 h^{2r+1},$$

or

$$|||e|||_h \le C\omega h^{r+\frac{1}{2}}.$$

This finishes the proof of the error estimate (30). □

Remark 5. *Typically, standard DG (without enrichment) with approximation u_{DG} would have (see, for example, ([7])*

$$|||e|||_h^2 \leq Ch^{r+\frac{1}{2}} \|U\|_{r+1,2,Q}.$$

Since $\|U\|_{r+1,2,Q} \sim \omega^{r+1}$ this error is dramatically larger than our error estimates (30).

6. Numerical Results

In this section, we will demonstrate some numerical experiments to verify our theoretical findings. Let us consider the scalar hyperbolic equation. We take $Q_T = \Omega \times (0,T] = [0, 2\pi] \times (0,T]$ and the initial condition

$$u(x, 0) = \sin(\omega x), \quad \omega = 100.$$

We choose the boundary conditions so that the exact solution is given by

$$u(x,t) = \sin(\omega(x - t)).$$

In this example, the initial condition has only one high frequency component so we take $L = 1$ and $n_1 \approx \omega$. For simplicity, we consider here only structured discretizations in space and time and choose $h = 2^{-\ell}, \quad \ell = 3, 4, 5, 6, 7$ and we use linear tensor-product polynomials, that is, $r = 1$. Thus we have 2 shape functions in the (unenriched) space-time DG space, and we have 6 shape functions (2 unenriched and 4 enriched) in the extended space-time DG space for the reference element $I^2 = (0, 1) \times (0, 1)$. Matrix integrals are all done on a reference element by using 10 Gauss-Lobatto points numerical integration. The most simple shape functions of maximum degree r in the reference element can be given by

$$\phi(\eta_0, \eta_1) = \eta_0^{r_0} \eta_1^{r_1}, \quad r = r_0 + r_1.$$

These shape functions give better conditioned mass and stiffness matrices, and make the computations relatively easier. Define the transformation

$$\begin{aligned} &G_K^n : (0, 1)^2 \to \mathcal{K}^n \\ &G_K^n(\eta_0, \eta_1) = (x, t), \end{aligned} \tag{34}$$

where

$$(x,t) = (\frac{1}{2}(t_n + t_{n+1}) - \frac{1}{2}(t_n - t_{n+1})\eta_0, \frac{1}{2}(1 - \eta_0)\xi_0 + \frac{1}{2}(1 + \eta_0)\xi_1)$$

with ξ_0 and ξ_1 are linear finite element shape functions that are the images of η_1 to the elements K^n and K^{n+1}, respectively, by a suitable mapping. An example of such a mapping, F_K^n can be given as

$$\begin{aligned} &F_K^n : I^2 \to K^n \\ &F_K^n(\eta_1) = \sum_{k=1}^{8} x_k(K^n) \chi_k(\eta_1), \end{aligned}$$

where $x_k(K^n)$ is the vertices of the element K^n and $\chi(\eta_1)$ is the standard linear finite element shape functions defined on I^2. Thus, the space-time tessellation consists of the union of all the partitioning of the space-time slabs. For more detailed discussions of such mappings and other basis functions, see [13] and [14]. The numerical results are shown in Table 1 and Table 2. The observed convergence rates (OCR) of the proposed method in L_2 and the energy norms are given at $T = 1$ and $T = 2$. The observed convergence rate R_1 in L_2 norm is computed by the formula $R_1 = \log(||e_{2h}||/||e_h||)/\log(2)$ and the observed convergence rate R_2 in the energy norm is computed by the formula $R_2 = \log(|||e_{2h}|||_h/|||e_h|||_h)/\log(2)$ where $e_h = u - U$ is the error on the mesh. It is known that optimal convergence is observed only by using suitable chosen meshes. The loss of order $h^{1/2}$ in the order of convergence of L_2 norm is still under discussion, e.g., see [32]. In practice, the optimal convergence h^{r+1} is achieved when polynomials of degree at most r used even if there is no uniform requirement on the chosen meshes. See [33] for the computational results for conforming triangulations for an example of this issue . Thus, typically there is a gap of order $h^{1/2}$ between computed convergence rate and the optimal convergence rate in DG methods.

h	$\|e_h\|_{L_2,T=1}$	R_1	$\|e_h\|_{L_2,T=2}$	R_1
1/8	0.2542	-	0.3653	-
1/16	0.7461e-1	1.739	1.070e-1	1.771
1/32	0.2193e-1	1.7664	0.288e-1	1.893
1/64	0.5993e-2	1.8715	0.768e-2	1.9068
1/128	0.1480e-2	2.0176	0.195e-2	1.9776

Table 1. The errors and the order of convergence of the space-time DG for the first order polynomial approximation ($r = 1$) at $T = 1$ and $T = 2$ in L_2 norm.

h	$\|\|\|e_h\|\|\|_{h,T=1}$	R_2	$\|\|\|e_h\|\|\|_{h,T=2}$	R_2
1/8	1.0532	-	1.2471	-
1/16	3.792e-1	1.473	4.584e-1	1.484
1/32	1.346e-1	1.494	1.563e-1	1.506
1/64	4.721e-2	1.511	5.491e-2	1.506
1/128	1.657e-2	1.510	1.943e-2	1.498

Table 2. The errors and the order of convergence of the space-time DG for the first order polynomial approximation ($r = 1$) at $T = 1$ and $T = 2$ in the energy norm.

The results in Table 2 clearly indicate that the numerical results are in good agreement with the theoretical findings and show that the proposed method convergences with the expected $(r+1/2)$-th order of convergence when the polynomial space of order r is used without any mesh refinement.

7. Conclusion

In this paper, we presented a space-time discontinuous Galerkin method for the scalar hyperbolic problems that contain high frequency components. We extend the space-time approximation space with trigonometric functions to capture the oscillatory behavior of the solutions. We applied discontinuous Galerkin methodology in both space and time and derived a stable space-time DG scheme. Thus, the method can be seen as a space-time framework of extended DG method. The key feature of the method is that it uses the solutions of PDE under consideration. Furthermore, the choice of DG space enriched by the solutions of the governing differential equation enables an efficient evaluation of integral terms. The proposed method here performs well when compared to standard space-time DG method. With conventional space-time DG method, one needs to refine the mesh size to get an acceptable accuracy for high frequency component. This leads to the computational costs in each space-time slab for solving the resulting system. We showed optimal a priori error estimates in a mesh dependent space-time DG norm. Additionally, we gave a numerical experiments to verify the theoretical findings. An extension of the analysis for an extended space-time solutions for the linear hyperbolic problems or conservation laws in two and three dimensional computational domains will be considered in the future.

Acknowledgements: The author would like to thank the anonymous reviewers for their valuable and constructive comments and suggestions that helped to improve the manuscript.

References

[1] Huttunen, J.M.J., Huttunen, T., Malinen, M. and Kaipio, J.P., Determination of heterogeneous thermal parameters using ultrasound induced heating and MR thermal mapping, *Phys. Med. Biol.*, 51 (2006), 1011-1032.

[2] Chirputkar, S.U. and Qian, D., Coupled Atomistic/Continuum Simulation based on an Extended Space-Time Finite Element Method, *CMES*, 850 (2008), 1-18.

[3] Garrido, P.L., Goldstein, S., Lukkarinen, J. and Tumulka, R., Paradoxial reflection in quantum mechanics (Preprint, 2008).

[4] Hughes, TJR., Franca, LP. and Mallet, M., A new finite-element formulation for Computational Fluid-Dynamics 6. Convergence analysis of the generalized SUPG formulation for linear time-dependent multidimensional advective-diffusive systems. *Computer Methods in Applied Mechanics and Engineering*, 63, (1987),97-112.

[5] Hulbert, GM. and Hughes, TJR., Space-time finite-element methods for 2nd-order hyperbolic-equations, *Computer Methods In Applied Mechanics And Engineering*, 84, (1990), 327-348.

[6] French, DA., A space-time finite element method for the wave equation, *Computer Methods in Applied Mechanics and Engineering*, 107, (1993),145-157.

[7] Johnson, C., Discontinuous Galerkin finite element methods for second order hyperbolic problems, *Computer Methods in Applied Mechanics and Engineering*, 107, (1993), 117-129.
[8] Grote, M. J., Schneebeli, A. and Schotzau D., Discontinuous Galerkin finite element method for the wave equation. *SIAM Journal on Numerical Analysis*, 44, (2006), 2408-2431.
[9] Johnson, C., Numerical Solutions of Partial Differential Equations by the Finite Element Method. Cambridge University Press, Cambridge, 1987.
[10] Falk, RS. and Richter, GR., Explicit finite element methods for symmetric hyperbolic equations, *SIAM Journal on Numerical Analysis*, 36, (1999), 935-952
[11] Monk, P. and Richter, GR., A discontinuous Galerkin method for linear symmetric hyperbolic systems in inhomogeneous media, *Journal of Scientific Computing*, 22-23, (2005), 443-477
[12] Demkowicz, L.F. and Gopalakrishnan, J., An overview of the discontinuous Petrovâ€“Galerkin method. *In Recent Developments in Discontinuous Galerkin Finite Element Methods for Partial Differential Equations*, Springer, (2014), 149-180.
[13] Van der Vegt, J.J.W. and Van der Ven, H., Space-time discontinuous Galerkin finite element method with dynamic grid motion for inviscid compressible flow, part I. General formulation, *J. Comput. Phys.* 182, (2002), 546-585
[14] Van der Vegt, J. J. W., Space-time discontinuous Galerkin finite element methods, *VKI Lecture Series. Von Karman Institute for Fluid Dynamics*, (2006), 1-37.
[15] Feistaur, M., Hajek, J. and Vadlenka, K.S., Space-time discontinuous Galerkin method for solving nonstationary linear convection-diffusion-reaction problems, *Appl. Math.,* 52, (2007), 197-234.
[16] Hulbert, GM. and Hughes, TJR., Space-time finite element methods for second-order hyperbolic equations. *Computer Methods in Applied Mechanics and Engineering*, 84, (1990), 327-348.
[17] Klaij, C., Van der Vegt, J.J.W. and Van der Ven, H., Space-time discontinuous Galerkin method for the compressible Navier-Stokes equations, *J. Comput Phys*, 217, (2006), 589-611.
[18] Sudirham, J.J., Van der Vegt, J.J.W. and Van Damme, R.M.J., Space-time discontinuous Galerkin method for advection-diffusion problems on time-dependent domains, *Appl. Numer. Math.* 56, (2006), 1491-1518.
[19] Feistaur, M., Kucera, V., Najzar, K. and Prokopova, J., Analysis of space-time discontinuous Galerkin method for nonlinear convection-diffusion problems, *Numer. Math.,* 117, (2011), 251-288.
[20] Rhebergen, S., Bokhove, O. and Van der Vegt, J.J.W., Discontinuous Galerkin finite element methods for hyperbolic nonconservative partial differential equations. *J. Comput. Phys.,* 227, (2008), 1887-1922.
[21] Ambati, V.R. and Bokhove, O., Space-time discontinuous Galerkin discretization of rotating shallow water equations, *J. Comput. Phys.,* 225, (2007), 1233-1261.
[22] Cessenat, O. and Despres, B., Application of an ultra weak variational formulation of elliptic pdes to the two-dimensional Helmholtz problem, *SIAM Journal on Numerical Analysis,* 35, (1998), 255-299.
[23] Banjai, L., Georgoulis, E.H. and Lijoka, O., A Trefftz polynomial space-time discontinuous Galerkin method for the second order wave equation, *SIAM J. Numer. Anal.,* 55(1), (2017), 63-86
[24] Farhat, C., Harari, I. and Franca, LP., The discontinuous enrichment method, *Computer Methods in Applied Mechanics and Engineering*, 190, (2001), 6455-6479.
[25] Chessa, J. and Belytschko, T., Arbitrary discontinuities in space-time finite elements by level sets and X-FEM, *International Journal for Numerical Methods in Engineering*, 61,(2014), 2595-2614.
[26] Moes, N., Dolbow, J. and Belytschko, T., A finite element method for crack growth without remeshing, *International Journal for Numerical Methods in Engineering*, 46, (1999), 131-150.

[27] Melenk, JM. and Babuska, I., The partition of unity finite element method: basic theory and applications, *Computer Methods in Applied Mechanics and Engineering*, 139, (1996), 289-314

[28] Toprakseven, S., Error Analysis of Extended Discontinuous Galerkin (XDG) Method. 2004, (Electronic Thesis or Dissertation). Retrieved from https://etd.ohiolink.edu/

[29] Johnson, C. and Pitkâranta, J., An analysis of the discontinuous Galerkin method for a scalar hyperbolic equation, *Math. Comp.,* 46, (1986), 1-26.

[30] Petersen, S., Farhat, C. and Tezaur, R., A space-time discontinuous Galerkin method for the solution of the wave equation in the time domain, *Int. J. Numer. Meth. Eng.,* 78, (2009), 275-295.

[31] Brenner, S.C. and Scott, L.R., The Mathematical Theory of Finite Element Methods, 3rd edn. Springer, New York, 2008.

[32] Cockburn, B., Dong, B. and Guzman, J., Optimal convergence of the original DG method for the transport-reaction equation on special meshes, Institute for Mathematics and its Applications, University of Minnesota, IMA Preprint Series, 2147 (2006).

[33] Richter, G. R., An optimal-order error estimate for the discontinuous Galerkin method, *Math.Comp.,* 50 (1988), 75-88.

Current address: Şuayip TOPRAKSEVEN: Faculty of Engineering, Department of Computer Science, Artvin Çoruh University, Artvin, Turkey.

E-mail address: `topraksp@artvin.edu.tr`

ORCID Address: `https://orcid.org/0000-0003-3901-9641`